Pure Appl. Geophys. 168 (2011), 1693–1706

DOI 10.1007/s00024-010-0194-x

Pure and Applied Geophysics

Seismic *b*-Value and the Assessment of Ambient Stress in Northeast India

PROSANTA KUMAR KHAN,[1] MANOJ GHOSH,[2] PARTHA PRATIM CHAKRABORTY,[3] and DEBDEEP MUKHERJEE[1]

Abstract—Seismicity data of northeast India, recorded between 1986 and 1999 by a local network, are analysed for estimation of *b*-values. Based on the obtained values, viz. low ($b \leq 0.5$), moderate ($0.5 < b \leq 0.7$) and high ($b > 0.7$), the study area is classified into different seismic-domains. An assessment of stress level is also carried out in identifying seismic-domains. Seismic activities, though mostly confined in some sectors, are presumably triggered by mutual interaction of the Shillong Plateau, Mikir Hills, Indo-Burman Ranges and the easternmost part of the Himalayas, and the contributions from deep-seated fractures cannot be ignored. The results resemble the seismic character of a foreland setting adjacent to a convergent margin. The *b*-values estimated for 240 square grids of dimension 0.6° × 0.6° over five seismic domains indicate wide variation. An analysis of cumulative seismic moment release (M_O) in different layers also indicates an anomaly in reference to the total seismic-energy budget of the five zones. The lower *b*-value and higher M_O recorded at relatively lower depth (~30 km) towards the southwest of the study area might be associated with upward bulging of a strong lithosphere. The bulging is perhaps regionally compensated by the downward flexing of the descending Indian lithosphere beneath the Upper Assam area; features unequivocally observed in any foreland setup. Towards the north and east of the study area, random variations of in both *b*-value and M_O along the converging zone suggest a varied tectonic environment with active interaction between the tectonic elements in these areas.

Key words: *b* Value, seismic moment energy, strong lithosphere, foreland, deep-seated fracture.

1. Introduction

Several studies have been carried out on the frequency–magnitude relationship of earthquakes as function of time, space, and depth since ISHIMOTO and IDA (1939) and GUTENBERG and RICHTER (1954), through their seminal works, established the empirical relationship between occurrence-frequency and magnitude of earthquakes in a given region for a finite time-window. Like many other self-organised and self-similar non-equilibrium systems, the earthquake magnitude–frequency relation follows an exponential relation, represented empirically by the equation

$$\text{Log } N(M) = a - bM \tag{1}$$

where $N(M)$ is the cumulative number of earthquakes having Richter magnitude larger than M, 'a' is a measure of seismic activity that depends on the size of the area, length of the observation period, the largest seismic magnitude and stress level of the area, etc., measured as the logarithm of the annual total of all earthquakes with $M > 0$ (ALLEN, 1986). Statistically, the *b*-value is the slope on the log $N \sim M$ regression line and is a constant parameter that determines the rate of fall in the frequency of occurrence of events with increasing magnitude. High *b*-values indicate a large number of small earthquakes expected in regions of low strength and large heterogeneity, and low *b*-values indicate high resistance (asperity) and homogeneity of the constituent rock-mass (TSAPANOS, 1990; UDIAS, 1999; WASON *et al*., 2002). In natural situations, *b*-values are found to lie between 0.5 and 1.5, depending on the tectonics of a region. MOGI (1963, 1967) and SCHOLZ (1968) studied the behaviour of *b*-values during fracturing of rocks in the laboratory. While the study of MOGI (1967) was mainly concerned with the mechanical behaviour of the rocks, SCHOLZ (1968) inferred that the state of stress, rather than the heterogeneity of the material constituting the rocks, plays the most important role in determining the

Electronic supplementary material The online version of this article (doi:10.1007/s00024-010-0194-x) contains supplementary material, which is available to authorized users.

[1] Department of Applied Geophysics, Indian School of Mines, Dhanbad 826 004, India. E-mail: pkkhan_india@yahoo.com; debdeep034@gmail.com

[2] Reliance Industries Limited, Seismic Data Acquisition and Processing Group, Mumbai, India. E-mail: manoj.ghosh@ril.com

[3] Department of Geology, University of Delhi, New Delhi 110007, India. E-mail: parthageology@gmail.com

b-value. Later studies (Mori and Abercrombie, 1997; Wiemer and Wyss, 1997) observed a decrease in *b*-value with increasing depth and related the observation with increasing applied stress at deeper levels (Bhattacharya and Kayal, 2003). The *b*-values also decrease with increasing effective stress or increasing seismic moment (M_O) release (Scholz, 1968; Wyss, 1973; Cao and Gao, 2002). In this paper we re-examine the distribution of *b*-values with depth for northeast India through a high resolution analysis using seismic data recorded at stations in a local network.

The study area lies between latitude 24.5°N and 27.2°N and longitude 89°E and 96°E, and is known for its strong seismic history. Although detailed investigations involving seismicity for the Shillong plateau as well as the whole of northeast India have been undertaken by several researchers (Verma *et al.*, 1976; Mukhopadhyay, 1984; Kayal, 1987; Kayal and Zhao, 1998; Radha Krishna and Sanu, 2000; Bilham and England, 2001; Bhattacharya *et al.*, 2008; Steckler *et al.*, 2008; Khan *et al.*, 2009), studies pertaining to the strength of the lithosphere and lithospheric-scale buckling are long-awaited for this convergent margin. Seismic *b*-values were analysed on a localised scale for appreciation of crustal heterogeneity (Kayal, 1987; Bhattacharya *et al.*, 2002, Bhattacharya and Kayal, 2003; Khan and Chakraborty, 2007). Geophysical tools such as seismic tomography and receiver functions were applied by Kayal and Zhao (1998) and Mitra *et al.* (2005) for identifying heterogeneities in the crust and upper mantle. Analysis of Bouguer and isostatic gravity anomalies (Verma and Mukhopadhyay, 1977; Chen and Molnar, 1990) led to the quantification of ~33–40 km crustal thickness for the Shillong Plateau area. Also, velocity structure and crustal configuration beneath northeast India were estimated on the basis of arrival time of local/teleseismic events (Tandon, 1954; Kayal and De, 1987; De and Kayal, 1990; Mukhopadhyay *et al.*, 1995; Rai *et al.*, 1999; Bhattacharya *et al.*, 2008). Depth-wise qualitative stress assessment beneath the Shillong Plateau area was carried out by Khan (2005a) and Khan and Chakraborty (2007). Despite all these advancements, documentation of *b*-value distribution in a space–depth framework over the entire area, recognition of anomalous patterns, if any, and identification of causative forcings are still awaited. The present study thus aims towards characterisation of space- and depth-wise *b*-value distribution over the entirety of northeast India and to understand the possible bearing of rheology/strength of the lithosphere on the *b*-value distribution pattern. Although we appreciate the limitations in '*b*' value estimation using available seismic catalogues (discussed later), we feel that the estimated *b*-values can be efficiently linked with the lithosphere strength profile in a depth domain (Molnar, 1988).

2. *Tectonic Setup*

Northward convergence, anticlockwise rotation against Eurasia and oblique convergence against the Southeast Asia (Dewey and Bird, 1970; Fitch, 1970; Seeber *et al.*, 1981; Le Dain *et al.*, 1984; Klootwijk *et al.*, 1985; Maung, 1987; Khan, 2005b) characterise the journey of the Indian plate since the Cretaceous period, and have led to the development of complicated tectonics in the northeast part of India. According to Curray (1989), the situation became even more complex near the syntaxis where the three plates viz., Indian, Eurasian and the Burma platelet, joined together and, accordingly, the deformational style changed from dextral shear, between India and Southeast Asia in the east, to a frontal collision at the eastern Himalayas. The entire northeast area has been tectonically active since the Mesozoic. Along with mountain building activities in the Burma and Himalaya regions in the east and north, large scale vertical movements resulted upliftment of the Shan plateau in Burma and the Shillong Plateau in northeast India (Krishnan, 1960). Interference of Shillong Plateau, Mikir Hill, Namcha Barwa Hill, Himalaya, Indo-Burman Ranges, etc., have resulted the development of a number of major crustal discontinuities, viz. Dauki Fault, Naga thrust, Kopili Lineament, and Main thrust-sheets in the northeast part of India (Fig. 1). As detached blocks from the Peninsular India Shillong plateau and Mikir Hills shifted over 200 km towards east through the gap between Rajmahal and Garo Hills (Evans, 1964), eastward motion of the Shillong Plateau along the transcurrent Dauki fault and the vertical tectonics of the entire

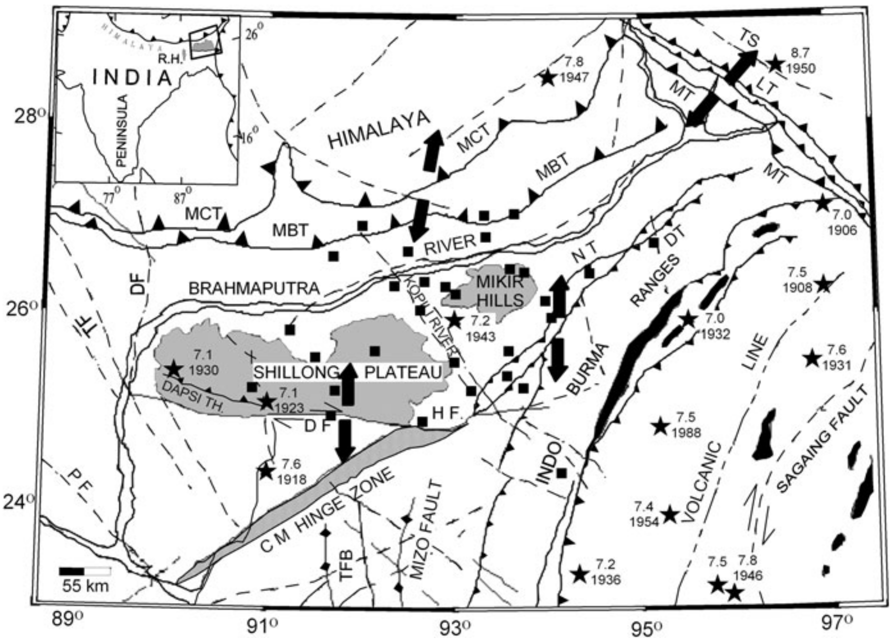

Figure 1
Map showing the tectonic setup of the northeast part of India (after Krishnan 1960; Evans 1964). *Inset map* represents the location of the study area. *DT* Disang thrust; *MBT* Main Boundary Thrust; *MCT* Main Central Thrust; *NT* Naga Thrust; *DF* Dauki Fault; *PF* Padma Fault; *TF* Tista fault; *HF* Halflong fault; *LT* Lohit thrust; *MT* Mishmi Thrust. The permanent seismic stations are shown by *solid squares*. *Solid stars* indicate the locations of historical large earthquakes. *Solid converging arrows* represent the direction of compressive stress field (after Radha Krishna and Sanu, 2000)

northeast region of India (Evans, 1964) led to the development of the complex tectonic setting in northeast India. The 1897 Shillong earthquake and 1950 Sadiya earthquake are explained as fallout of the southward movement of the Shillong Plateau at the last phase of Himalayan orogeny and oblique convergence of the Indian plate against the Burmese micro-plate, respectively (Evans, 1964; Ben Menahem *et al*., 1974).

The combined gravitational, aeromagnetic and seismic data indicate that a buried ridge represents the basement below the alluvial cover of Upper Assam and the ridge extended towards the northeast (Verma and Mukhopadhyay, 1977; Kent and Dasgupta, 2004; Mitra *et al*., 2005). To the northern part of the Shillong Plateau, the basement of the Lower Assam Valley is exposed as low-lying ridges on either side of the Brahmaputra River. Satellite imagery (Nandy and Dasgupta, 1986) shows a number of buried lineaments beneath the alluvium in the Lower Assam Valley. The Shillong plateau is separated from the western part of the Surma valley by a narrow strip of southerly dipping beds associated with an important E–W discontinuity, the Dauki fault. The Disang thrust, southwest of Naga Hills, passes to a narrow but complex fracture belt near Haflong, i.e., the Haflong fault. With change in orientation from NE–SW to due west (Evans, 1964), the fracture belt continues westward up to the Dauki fault.

3. Seismic Data and Methodology

The seismological observatory network in northeast India was constructed jointly by the National Geophysical Research Institute (NGRI), Hyderabad, and the Regional Research Laboratory (RRL), Jorhat, in the 1980s (Bhattacharya *et al*., 2002; Bhattacharya and Kayal, 2003; Bhattacharya *et al*., 2008), and has been recording local seismicity for more than two decades. The earthquake data used for the present study were collected from the earthquake catalogues published by the NGRI, Hyderabad, and RRL, Jorhat.

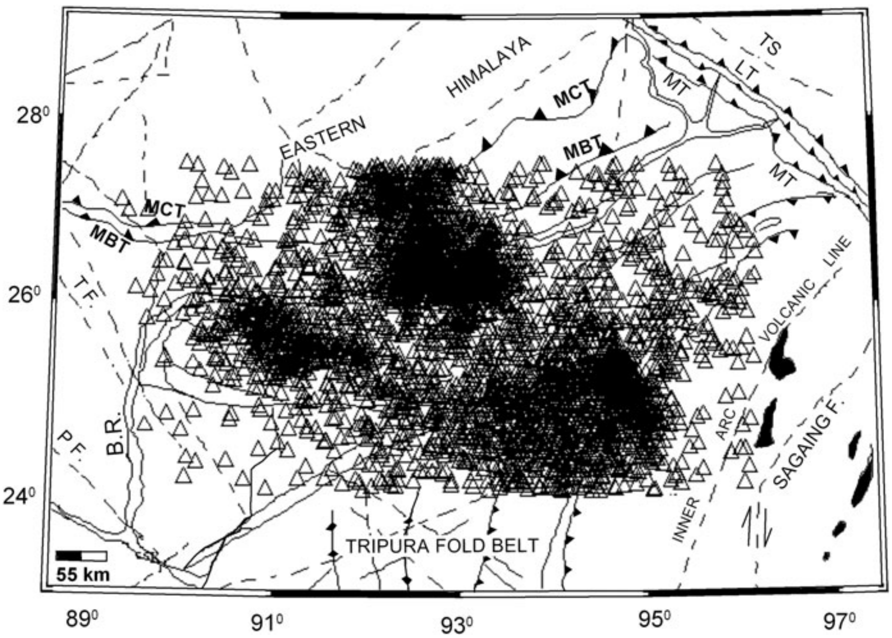

Figure 2
Map showing seismicity in Northeast India occurring between 1986 and 1999, and recorded by the local network of National Geophysical Research Institute (NGRI), Hyderabad, and Regional Research Laboratory, Jorhat

These catalogues incorporate the events recorded by the NGRI and RRL networks containing 30 digital stations and also the data recorded by temporary local networks' digital seismic stations ($\sim$47) run by different institutes in different times and places; these stations were not in operation at a single time in the northeast region. The over all timing accuracy for the temporary stations was maintained to $\pm$0.1 s synchronizing radio signal (Kayal, 1987; Kayal and De, 1991). The timing for the digital seismic stations, is however, maintained by GPS. The three component digital seismograms provided high precision P-wave ($\pm$0.01 s) and S-wave ($\pm$0.05 s) arrival times. The catalogues generally are completed for the most part down to magnitude 2.0. In the present study we have used the network duration magnitude for an earthquake. Under this measure, the magnitude for an earthquake is determined from the arithmetic mean of duration magnitudes over different stations. A total of 3,655 events occurring in the areas between latitude 24.2°N and 27.5°N and longitude 89.3°E and 96.2°E (Fig. 2) during the period between 1986 and 1999 were used. An extended rectangular area surrounding the main study region was considered to include the analysed *b*-values along the peripheral zone for high-resolution investigation.

The study area (Fig. 1) was divided into 240 square grids for exploring the spatial variation of *b*-values over the region. Each grid has a dimension of 0.6° × 0.6° (geographical window) with a moving window (overlapping area) of 0.3° × 0.3°. The moving window was chosen for comprehensive analysis and to maintain the inherent grid-to-grid continuity of the data points. The dimension of the geographic window under the present study was selected to introduce an adequate number of events representing the *b*-values at each grid. A few squares with poor event records (Table 1 in Electronic Supplementary Material) were excluded from the analysis. Some other squares which lack sufficient events (occasionally $<$30) are, however, considered for maintaining good correspondence between projection points in adjacent grids. For a defined magnitude range, *b*-values for each block were computed using Eq. 1.

Figure 3 illustrates the computed *b*-values from cumulative frequency–magnitude relationships for four grid squares. The plots ubiquitously show

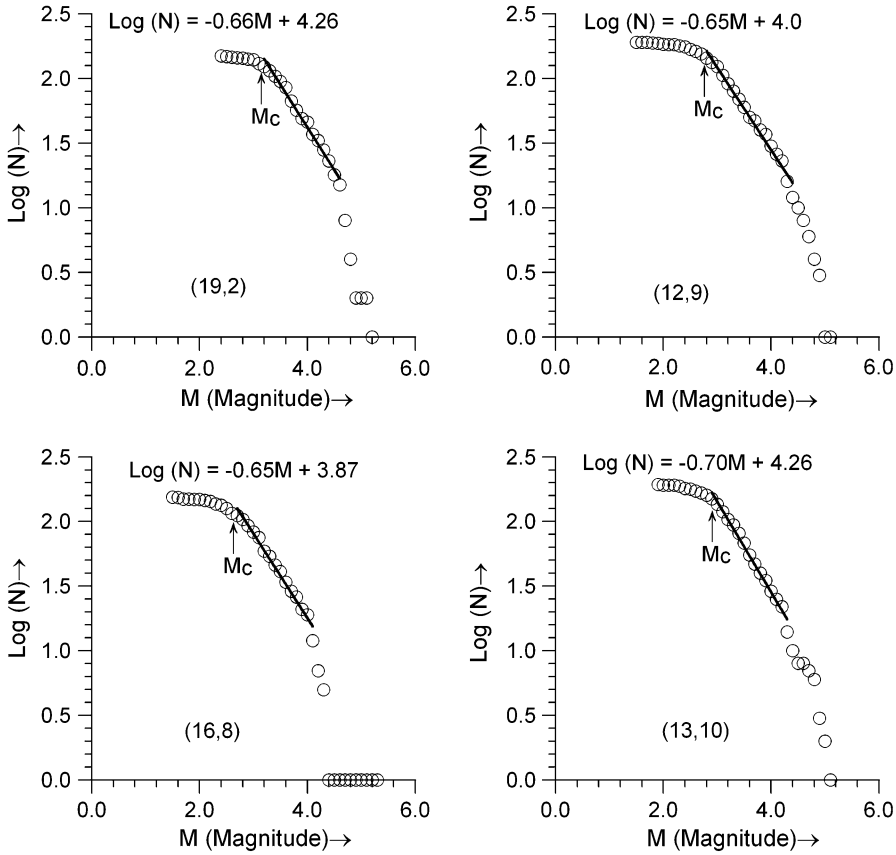

Figure 3
Diagram showing the variation of cumulative frequency with earthquake magnitude for four seismic blocks (19, 2), (16, 8), (12, 9) and (13, 10), respectively. Selection of best fit lines is explained in the *text*. *Arrows* mark the smallest magnitude at which the distribution in the respective grid is complete

deviations from linearity at both higher and lower ends of the data values. While the deviations in the higher end may be accounted for by scarcity of large magnitude (M) events within the considered time-window (1986–1999 i.e. ~15 years), the deviations in the lower data values may be due to incompleteness in the data catalogue. Such heterogeneity in the data catalogue, particularly in the lower data range, may stem from (1) lack of enough stations to record very small events (2) disinterest of network operators in recording events below a certain threshold or (3) non-random aftershock events which may be too small to be detected within the code of larger events. Several workers (Weimer and Wyss, 2000; Woessner and Weimer, 2005) have discussed this limitation and have stressed the requirement of minimum magnitudes for complete recording (M_c) in studies related to seismicity. Despite the understanding that M_c may change with time in most catalogues for different regions, usually decreasing with increase in the number of seismographs and improvement in the methods of analysis, it is widely and effectively practised in literature for b-value assessment of high seismic areas (Rydelek and Sacks, 1989; Weimer and Wyss, 2000). Since the area under study is seismically very active, we pursued our study with demarcation of M_c (i.e. lower bound of MRBE in Table 1 in Electronic Supplementary Material) on the cumulative frequency–magnitude database (Fig. 3) based on the points at which the b-value departs from linearity (cf. Rydelek and Sacks, 1989). The b-values we estimated are restricted to a dataset that shows the self-similar character (cf. Pacheco *et al.*, 1992) without any significant modulation. Further, we have carried out the exercise of estimating the root mean square error (RMSE) in reference to the predicted

Table 1

Values of the parameter b computed at different depths for seismic zone I, II, III, IV, V

Serial no.	Depth ('h' in km)	Projection point (depth in km)	b value	N	N_0	MRAE	MRBE	Percentage (%) of events used $\left[\left(\frac{N_0}{N}\right) \times 100\right]$	RMSE
Zone I									
1	$0.0 \le h < 12.0$	6.0	0.32	14	11	2.0–5.1	2.5–4.7	78.87	0.06
2	$6.0 \le h < 18.0$	12.0	0.57	25	19	2.2–5.1	2.8–4.8	76.00	0.07
3	$12.0 \le h < 24.0$	18.0	0.77	41	28	2.1–5.4	3.0–4.3	68.29	0.07
4	$18.0 \le h < 30.0$	24.0	0.68	38	25	2.1–5.4	3.0–4.6	65.78	0.04
5	$24.0 \le h < 36.0$	30.0	0.43	20	15	2.7–4.9	3.1–4.6	75.00	0.06
6	$30.0 \le h < 42.0$	36.0	0.43	16	12	3.1–4.7	3.3–4.4	75.00	0.03
7	$36.0 \le h < 48.0$	42.0	0.53	14	11	2.6–4.4	2.9–3.7	78.57	0.03
8	$42.0 \le h < 54.0$	48.0	0.62	91	69	1.8–5.4	3.0–4.8	75.82	0.06
Zone II									
1	$0.0 \le h < 12.0$	6.0	0.81	96	61	1.0–4.5	3.0–4.2	63.54	0.05
2	$6.0 \le h < 18.0$	12.0	0.86	187	161	1.0–4.8	2.6–4.3	86.10	0.07
3	$12.0 \le h < 24.0$	18.0	0.73	319	257	1.1–5.4	2.6–4.8	80.56	0.05
4	$18.0 \le h < 30.0$	24.0	0.65	276	266	1.1–5.4	2.6–4.7	96.38	0.04
5	$24.0 \le h < 36.0$	30.0	0.46	90	85	1.1–5.0	1.9–4.7	94.44	0.10
6	$30.0 \le h < 42.0$	36.0	0.96	58	50	1.5–5.4	3.3–4.9	86.21	0.07
7	$36.0 \le h < 48.0$	42.0	0.70	53	39	2.1–5.4	3.0–4.2	73.58	0.08
8	$42.0 \le h < 54.0$	48.0	0.57	25	20	2.1–4.3	2.9–4.0	80.00	0.05
Zone III									
1	$0.0 \le h < 12.0$	6.0	0.56	94	89	1.1–5.2	1.8–4.8	94.68	0.05
2	$6.0 \le h < 18.0$	12.0	0.67	155	108	1.1–5.2	2.5–4.4	69.68	0.05
3	$12.0 \le h < 24.0$	18.0	0.70	316	235	1.0–4.9	2.5–4.3	74.37	0.06
4	$18.0 \le h < 30.0$	24.0	0.64	326	280	1.0–5.0	2.3–4.5	85.89	0.09
5	$24.0 \le h < 36.0$	30.0	0.62	173	119	1.5–5.3	2.7–4.9	68.79	0.05
6	$30.0 \le h < 42.0$	36.0	0.61	143	118	1.6–5.3	2.5–4.8	82.52	0.05
7	$36.0 \le h < 48.0$	42.0	0.73	146	114	1.8–5.2	2.8–4.8	78.08	0.70
8	$42.0 \le h < 54.0$	48.0	0.59	97	89	1.8–5.2	2.5–4.8	91.75	0.08
Zone IV									
1	$0.0 \le h < 12.0$	6.0	0.93	111	91	1.7–4.8	2.8–4.6	81.98	0.07
2	$6.0 \le h < 18.0$	12.0	1.12	240	211	1.7–5.2	3.0–4.8	87.92	0.06
3	$12.0 \le h < 24.0$	18.0	1.14	563	376	1.4–5.2	3.0–5.0	66.79	0.10
4	$18.0 \le h < 30.0$	24.0	0.99	593	410	1.4–5.7	3.0–5.1	69.14	0.09
5	$24.0 \le h < 36.0$	30.0	0.66	288	235	1.7–5.7	2.8–4.6	81.60	0.06
6	$30.0 \le h < 42.0$	36.0	0.93	242	159	1.8–5.3	3.2–4.6	65.70	0.05
7	$36.0 \le h < 48.0$	42.0	0.75	251	187	1.6–6.2	3.0–4.3	74.50	0.07
8	$42.0 \le h < 54.0$	48.0	0.79	153	112	1.6–6.2	3.2–5.1	73.20	0.08
Zone V									
1	$0.0 \le h < 12.0$	6.0	0.58	58	42	2.6–4.7	3.0–4.7	72.41	0.03
2	$6.0 \le h < 18.0$	12.0	0.60	107	80	2.5–5.2	3.1–4.6	74.77	0.04
3	$12.0 \le h < 24.0$	18.0	0.79	214	151	1.7–5.2	3.3–4.7	70.56	0.04
4	$18.0 \le h < 30.0$	24.0	0.77	234	179	1.7–5.2	3.2–4.7	76.50	0.08
5	$24.0 \le h < 36.0$	30.0	0.67	125	98	2.2–5.3	3.2–4.8	78.40	0.05
6	$30.0 \le h < 42.0$	36.0	0.46	100	87	2.3–5.3	2.9–4.6	87.00	0.08
7	$36.0 \le h < 48.0$	42.0	0.93	130	70	2.7–5.2	3.4–4.6	53.85	0.10
8	$42.0 \le h < 54.0$	48.0	0.80	131	107	2.2–5.1	3.3–5.0	81.68	0.09

best fit line over the self-similar dataset, which enhanced the degree of accuracy of the estimated b-values. We agree that the present entire exercise has narrowed down the considered database (Table 1 in Electronic Supplementary Material; Table 1), but at the same time, confining our study to a self-similar dataset where the catalogue is complete (Fig. 3) placed the estimated 'b' values on very strong footing.

On the map, the estimated b-value for each square grid was spatially assigned to a point that defined the intersection of two diagonals of the square block; the

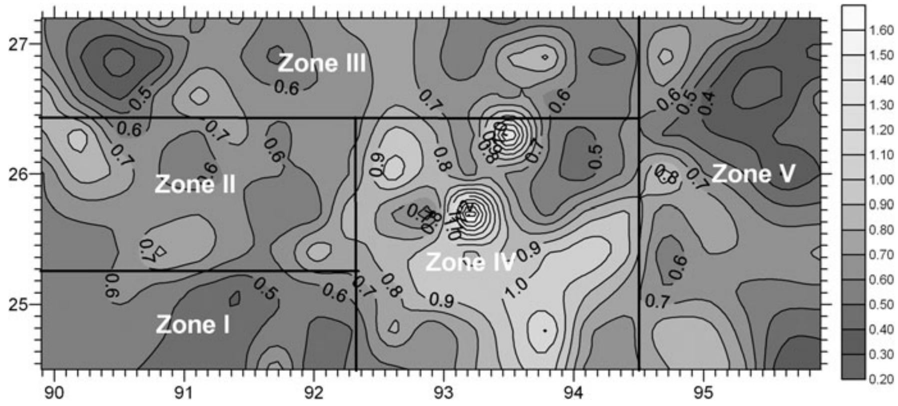

Figure 4
b-Value contour map for the northeast India. Contour interval is 0.1. Different seismic zones (demarcate by *solid lines*) were classified based on *b*-values

projected values were then used for *b*-value mapping over the entire study area (Fig. 4). Based on a comparative analysis of *b*-value contours, five broad zones (Zones I–V) of nearly uniform *b*-values were identified, and depth probing of *b*-values was carried out at different layers with 12 km thickness, starting from surface down to 54 km depth (Table 1 in Electronic Supplementary Material) for understanding the intra- and inter-zone variations in *b*-values with respect to depth. An overlapping layer of 6 km thickness (moving depth-window) was considered for maintaining inherent continuity of the data points, minimization of depth error and observation at high-resolution. Further, the total seismic moment energy ($\sum M_O = 10^{(1.53 m_b + 16.17)}$, M_O seismic moment energy for each layer, m_b body wave magnitude) released in each zone was estimated and a comparative assessment of M_O carried out between layers for individual zones.

4. Results

Overall, the *b*-values are widely spreaded (Fig. 4) over the northeast part of India. The minimum and maximum estimated *b*-values in the study area are 0.23 and 1.78, respectively (Table 1 in Electronic Supplementary Material; Table 1); maximum concentration around 0.6 (Fig. 5). Based on the distribution (Fig. 5), *b*-values were classified into three categories; viz. low ($b \le 0.5$), moderate ($0.5 < b \le 0.7$) and high ($b > 0.7$). High resolution observation reveals sectorial preference of values, e.g., low *b* values (0.4–0.6) in the southwest, eastern part of ~95.2° longitude, and northwest, comparatively higher values (~0.5–1.6) in the central part between latitudes 24.5°N and 26.5°N and longitudes 92.3°E and 94.5°E. For understanding the vertical strength (Molnar, 1988; Watts and Burov, 2003) variation within the lithosphere of the study area, the estimated *b*-values over a 54 km thickened single-layer were further critically analyzed. Considering the available concentration of earthquake event data and necessity of depth probing, the *b*-values were assessed for comparatively thinner slices (of 12 km thickness) in each contoured zone (Fig. 4). To understand the role of different deep-seated geomorphic features on earthquake incidences, analysis of seismic moment release was also carried out in each layer of the five specific zones (Fig. 6). Maximum energy release amounts to 1.66×10^{26} dyne-cm in Zone IV; successively lesser amounts are recorded in other zones viz. 1.30×10^{25} dyne-cm in Zone I, 1.09×10^{25} dyne-cm in Zone II, 3.78×10^{25} dyne-cm in Zone III and 5.64×10^{25} dyne-cm in Zone V.

The five zones (Zones I–V) can now be characterized spatially in terms of seismic *b*-values (Fig. 7) and moment energy release (Fig. 6). Zone I documents low to moderate *b*-values, and the highest seismic moment energy was released through a crustal domain (i.e., ~25 and 36 km depths) where the lower *b*-values were recorded. Zone II documents,

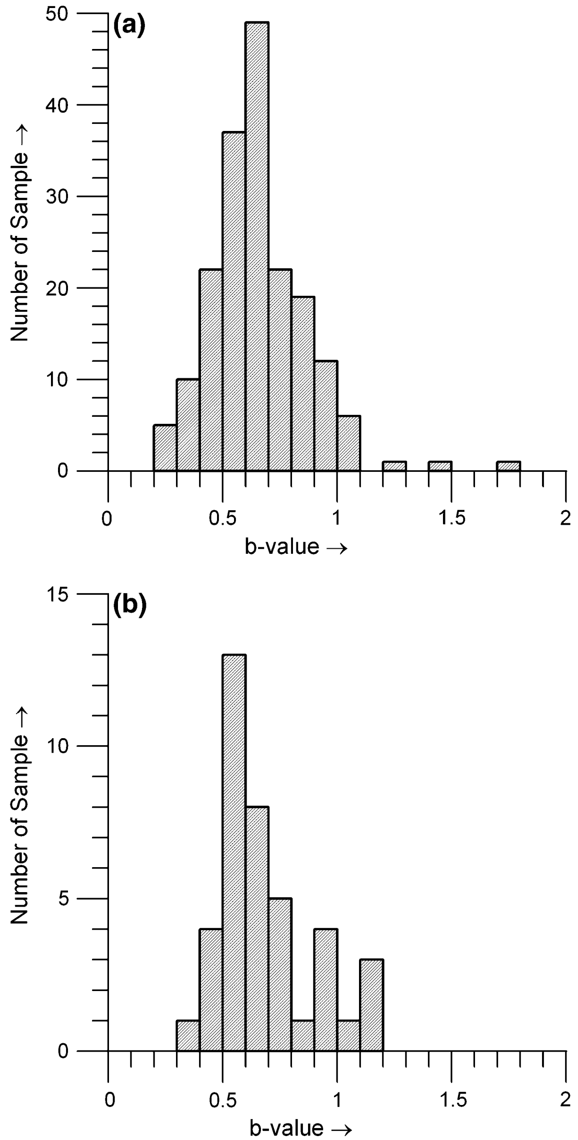

Figure 5
Histogram plots showing the variation of frequency of *b*-values over the entirety of northeast India (**a**) and over five zones (**b**)

overall, a moderate *b*-value with the lowest *b*-value noted at a depth of 30 km, and the highest moment energy release at comparatively greater depths (∼40 km). Zone III documents moderate to low *b*-values, and maximum moment energy released through a domain at depths between 30 and 40 km, whereas the lowest *b*-value was recorded at a depth of 36 km. Although the different layers document low to moderate *b*-values, distribution is more or less non-uniform. Zone IV records moderate to high *b*-values, and high seismic moment energy release at >40 km depth, whereas the lowest *b*-value was recorded at a depth of 36 km. The *b*-values are moderate to low in Zone V. The *b*-values were non-uniformly distributed over the entire depth range; the lowest value was recorded at a depth of 36 km, and the maximum moment was released through a thickened layer between ∼20 and 36 km in depth. Depths of higher seismic moment release are not uniform in all zones, and, particularly, a depth-domain (i.e., ∼25–40 km) in Zones I, II and III registered the maximum amount of seismic moment release. By contrast, Zones IV and V are odd in this category. The *b*-values are, however, observed to be lowest at depths between ∼30 and 36 km in all the zones. A good correspondence between the lowest *b*-value and the higher seismic moment release was noted invariably in the mid-crustal domain of all the zones, and might be indicative of a sharp change in rheology within the continental lithosphere (Molnar, 1988). The higher *b*-values recorded at the shallower part of the lithosphere in all the zones might be associated with more heterogeneous crustal domain at the base of the upper crust.

5. Discussion and conclusions

Widely varying stress in space–depth frame, modified by subsurface heterogeneities (structural/rheological), account for uneven distribution of seismicity in northeast India. More variable *b*-values in Zones III and V (Fig. 7) perhaps suggest the presence of fractures at different depth-levels along the eastern and northern boundaries of northeast India. Possibly, a substantial amount of ambient tectonic stress gets dissipated in form of earthquakes along the Himalaya and Indo-Burman Ranges, and the remaining part is utilised for enhancing the stress field towards the interior of the northeast part of India. It thus may be proposed that deep-seated fracture zones evolved from continued subduction of the Indian lithosphere towards the north and northeast, and concomitant synorogenic movements in the Himalaya and Indo-Burma Ranges exert significant influence on the seismicity of the area (Evans, 1964; Verma and Mukhopadhyay, 1977). Numerous Hills, elevated lands and flat valleys, which evolved through vertical

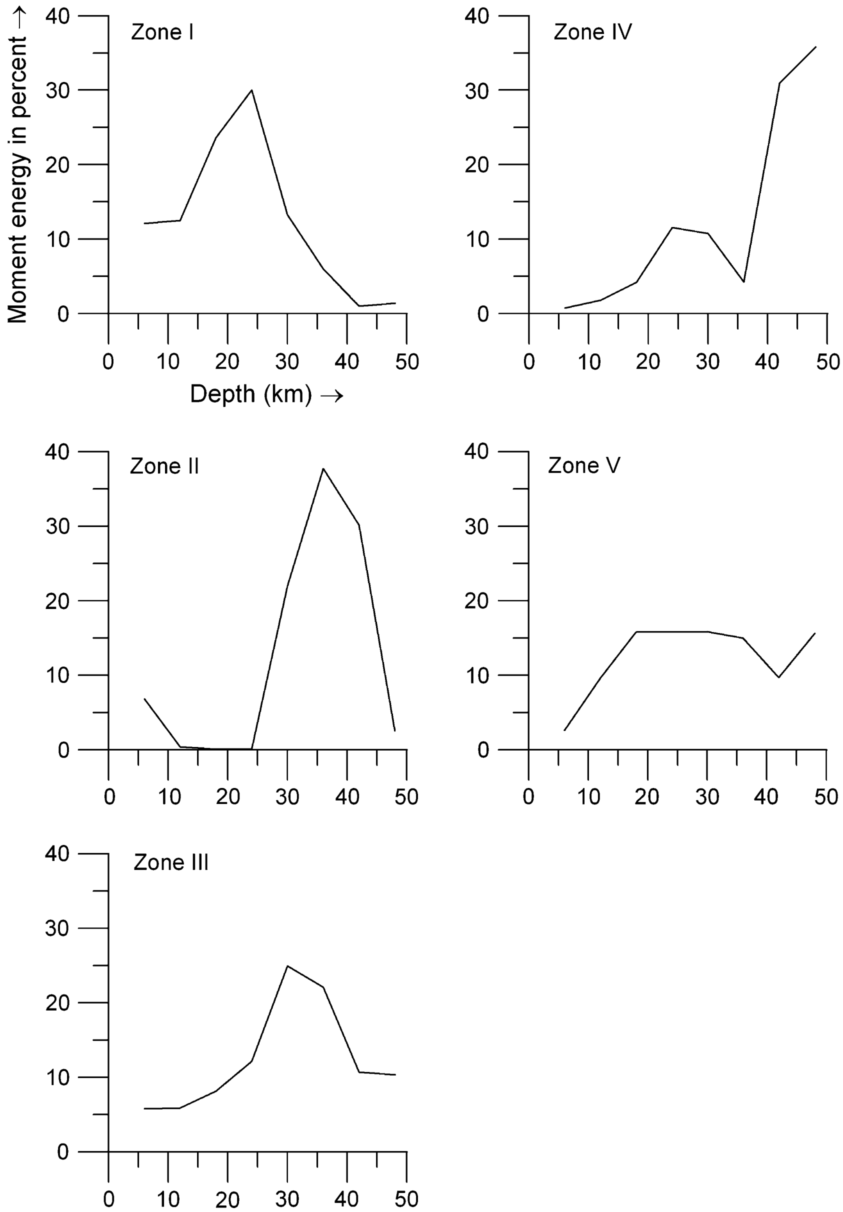

Figure 6
Plots showing the depth-wise variation of percentage of seismic moment (M_o) released through the five zones

tectonics (EVANS, 1964), also partially influence the seismic activities of the area. High seismicity with high b-values is commonly associated with a high degree of crustal heterogeneity (LOWRIE, 1997; WASON *et al.*, 2002), and corroborates the above observation. Structural complexity, including thrust sheets in the north and east and criss-crossing high-density faults/lineament systems are very common features of northeast India (NANDY, 1980). Seismic zones with high b-values in some pockets in the western part of the study area can possibly be related to the presence of high density rock-fractures resulting from strong tectonisation between the Himalaya and the Shillong Plateau (cf. KHAN and CHAKRABORTY, 2007). The relatively higher b-values in Zone IV may be the result of mutual interaction between the Shillong Plateau, Mikir Hills, Kopili Lineament and the Indo-Burman Ranges.

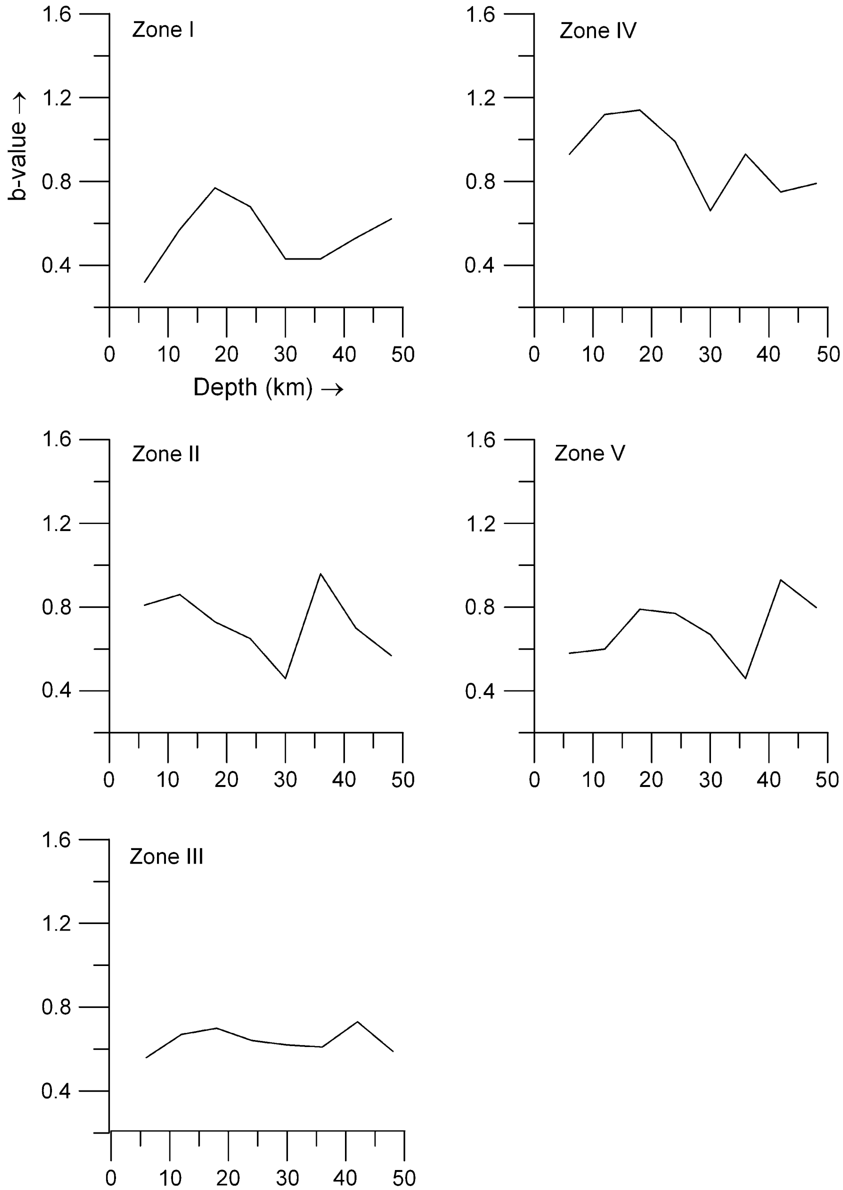

Figure 7
Plots showing the depth-wise variation of *b*-values for the five zones

The lower *b*-values and relatively high seismic moment release in the mid-crustal domain beneath the southwestern part of the study area (Figs. 2, 6, 7) may be better understood in terms of rheological anomaly, presen, though unambiguous, in parts of northeast India. Modification of the stress field as a result of continuing interaction of northeast India with the Himalaya and Indo-Burman Ranges is also another dominant process, particularly noted along its northern and eastern boundaries. Positive Bouguer anomaly as high as ~+40 mGal (Fig. 8) and isostatic anomaly ~+100 mGal (Fig. 9) recorded in the southwest part of the area were explained by overcompensation of the Shillong Plateau and Mikir Hills (Chen and Molnar, 1990). In contrast, Bouguer gravity as low as ~−260 mGal and isostatic anomaly ~−125 mGal in the northeastern part clearly argue for a state of undercompensation in the

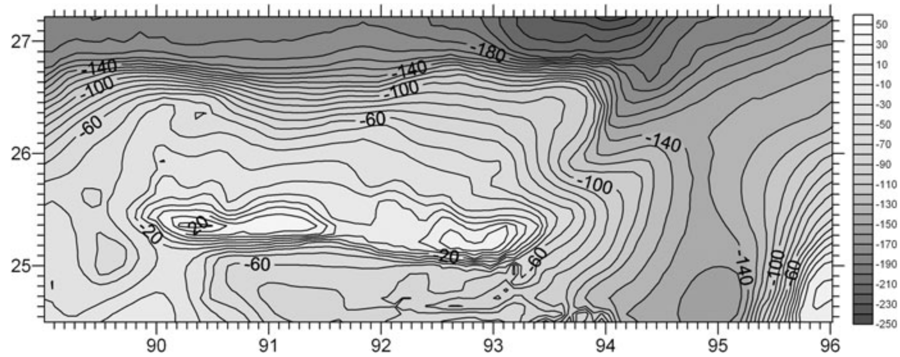

Figure 8
Bouguer gravity anomaly contour map for northeast India (after VERMA and MUKHOPADHYAY, 1977). Contour interval is 10 mGal. Note the wide variation of Bouguer gravity from ∼+40 mGal over Shillong Plateau to ∼−260 near Upper Assam

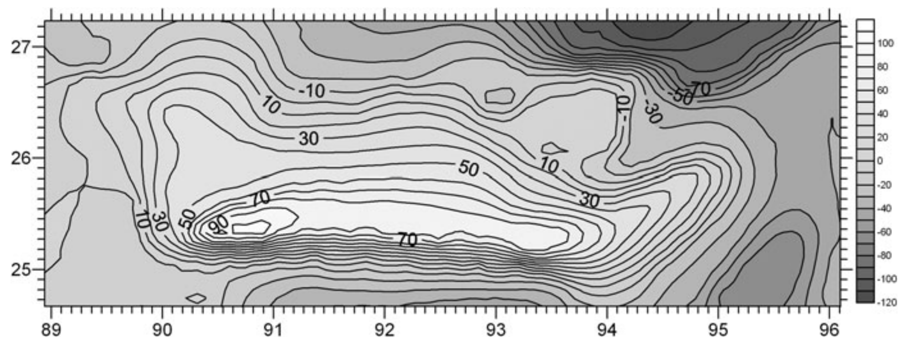

Figure 9
Isostatic anomaly map of the study area (after VERMA and MUKHOPADHYAY, 1977). Contour interval is 10 mGal. Note the wide variation of isostatic gravity anomaly from ∼+100 mGal over Shillong Plateau to ∼−125 near Upper Assam

foreland of upper Assam area. The resultant isostatic imbalance near the foothills is possibly accommodated through flexural bulging beneath the Shillong Plateau area. This broad sub-surface trend is normally a typical feature observed at convergence margins where collisional orogens with five tectonic components, viz. thrust belts, foreland flexures, plateaux, widespread foreland deformational zones, and zones of orogenic collisional collapse, are ubiquitous worldwide (CONDIE, 1997; KHAN *et al*., 2010). It is thus inferred that the positive compensation towards the southwestern part is caused by the elevated descending Indian lithosphere (e.g., lithospheric-scale buckling, cf. RODGERS, 1987), whereas low *b*-value and high seismic moment release can be linked with a higher level of stress. The proposed active deformation of the uprising Shillong–Mikir massif (a fragmented portion of the Indian shield, MUKHOPADHYAY, 1984) with crustal thickening of ∼2.4 mm/year (RADHA KRISHNA and SANU, 2000) is possibly linked with incidence of the great 1897 Assam earthquake (BILHAM and ENGLAND, 2001).

A quantitative appreciation of the earthquake record over a time window may sometimes offer clues, not only for understanding the long-term lithosphere deformation, but also the constitution of the continental crust at any particular region in terms of different rheological domains (MEISSNER and STREHLAU, 1982; CHEN and MOLNAR, 1983; KIRBY and KRONENBERG, 1987). Though it has been postulated that the lower crust in continental areas is devoid of any seismic activity because of its higher geothermal condition and lower strength (cf. CHEN and MOLNAR, 1983), the recorded seismicity at greater depth in northeast India can possibly be correlated with lower heat flow (cf. THUSSU, 2002), as usually observed in shield areas and platforms. Further, the crustal strength with depth varies with tectonic setting, strain rate, thickness and composition. In settings with lower geothermal energy, brittle fractures may be continued up to the lower crust level or further below into the upper mantle because mafic and ultramafic rocks can behave in a very resistive manner to plastic failure (Rutter and Brodie, 1992). Indeed, mantle deformation is speculated at more than ~40 km depth beneath the northeast India on the basis of observation of seismicity (Chen and Molnar, 1990). Combining the observations, e.g., positive Bouguer gravity and isostatic anomalies, lowest *b*-value and high seismic moment release in the southwestern part of the study area (i.e., Zone I) we propose down-buckling of the descending Indian lithosphere. The related flexural upbulging is presumably being accommodated beneath the Upper Assam area. This is also supported by the observed Bouguer gravity and isostatic anomalies in those areas (discussed before). The downward lithosphere-scale buckling (Burg and Podladchikov, 1999) is considered coeval with the block uplift of the Naga Hills on the SE, Mishmi Hills and Assam syntaxis on the NE and Mikir Hills and Shillong Plateau on the SSW (Verma and Mukhopadhyay, 1977) of the study area. The contention is also supported by the work of Chen and Molnar (1990), which postulated the existence of a subducting strong lithosphere beneath the Shillong plateau.

Acknowledgments

The first author is thankful to the Director, Indian School of Mines, Dhanbad for providing the infrastructure facilities. PPC acknowledges the infrastructural help extended by the Department of Geology, Delhi University. The authors are thankful to two anonymous referees for critical comments and suggestions, which improved our manuscript. This work has been supported partially by the grants from MRP, ISM, Dhanbad and partially by the Ministry of Earth Sciences, Govt. of India, New Delhi.

References

Allen, J.R.L. (1986), *Earthquake magnitude-frequency, epicentral distance, and soft-sediment deformation in sedimentation basins*, Sediment. Geol. 46, 67–75.

Ben Menahem, A., Aboodi, E., and Schild, R. (1974), *The source of great Assam earthquake an interplate wedge motion*, Phys. Earth Planet. Int. 9, 265–289.

Bhattacharya, P.M., Majumder, R.K., and Kayal, J.R. (2002), *Fractal dimension and b-value mapping in northeast India*, Curr. Sci. 82, 1486–1491.

Bhattacharya, P.M., and Kayal, J.R. (2003), *Mapping the b−values and its correlation with the fractal dimension in the northeast region of India*, J. Geol. Soc. India 62, 680–695.

Bhattacharya, P.M., Mukhopadhyay, S., Majumdar, R.K., and Kayal, J.R. (2008), *3-D seismic structure of the northeast India region and it simplications for local and regional tectonics*, J. Asian Earth Sci. 33, 25–41.

Bilham, R., and England, P. (2001), *Plateau pop-up in the 1897 Assam earthquake*, Nature 410, 806–809.

Burg, J.-P., and Podladchikov, Yu. (1999), *Lithospheric scale folding: numerical modeling and application to the Himalayan syntaxes*, Int. J. Earth Sci. 88, 190–200.

Cao, A., and Gao, S.S. (2002), *Temporal variation of seismic b−values beneath north-eastern Japan island arc*, Geophys. Res. Lett. 29, 48, 1−3.

Chen, W.-P., and Molnar, P. (1983), *Focal depths of intracontinental and intraplate earthquakes and their implications for the thermal and mechanical properties of the lithosphere*, J. Geophys. Res. 88, 4183–4214.

Chen, W.P., and Molnar, P. (1990), *Source parameters of earthquakes beneath the Shillong Plateau and the Indoburman ranges*. J. Geophys. Res. 95, 12527–12552.

Condie, K.C. (1997), *Plate Tectonics and Crustal Evolution*, Butterworth-Heinemann, Great Britain.

Curray, J.R. (1989), The Sunda arc: A model for oblique plate convergence, *In* Symposium, Snellius II Expedition, Jakarta, Geology and Geophysics of the Banda Arc, Van Hinte, J.E., van Weering, Tj.c.e., and Fortuin, A.R. Eds: (Neth. J. Sea. Res., 24) pp. 131–140.

De, R., and Kayal, J.R. (1990), *Crustal P-wave velocity and velocity-ratio study in northeast India by a microearthquake survey*, Pure Appl. Geophys. 134, 93–108.

Dewey, J.F., and Bird, J.M. (1970),*Mountain Belts and Global tectonics*, J. Geophys. Res. 75, 2625−2647.

Evans, P. (1964), *The tectonic frame work of Assam*, J. Geol. Soc. India 5, 80–96.

Fitch, T.J. (1970), *Earthquake mechanism in the Himalayan, Burmese and Andaman region and continental tectonics in Central Asia*, J. Geophys. Res. 75, 2699–2709.

Gutenberg, B., and Ritcher, C.F. (1954), *Seismicity of the earth and associated phenomenon*, Princeton University press. Pinceton.

Ishimoto, M., and Ida, K. (1939), *Observations sur les seisms enregistre par le microseismograph construit dernierment*, Bull. Earthquake Res. Inst., Tokyo Univ. 17, 443–478.

Kayal, J.R. (1987), *Microseismicity and source mechanism study: Shillong Plateau, northeast India*, Bull. Seismol. Soc. Am. 77, 184–191.

KAYAL, J.R., and DE, R. (1987), *Pn velocity study using a temporary seismograph Network in the Shillong Plateau, northeast India*, Bull. Seismol. Soc. Am 77, 1718–1727.

KAYAL, J.R., and DE, R. (1991), *Microseismicity and tectonics in northeast India*. Bulletin of Seismological Society of America 81, 131–138.

KAYAL, J.R., and ZHAO, D. (1998), *Three−Dimensional Seismic Structure beneath Shillong Plateau and Assam Valley, Northeast India*, Bull. Seismol. Soc. Am 88, 667–676.

KENT, W.N., and DASGUPTA, U. (2004), *Structural evolution in response to fold and thrust belt tectonics in northern Assam. A key to hydrocarbon exploration in the Jaipur anticline area*, Mar. Petroleum Geol. 21, 785–803.

KHAN, P.K. (2005a), *Mapping of b-value beneath the Shillong Plateau*, Gond. Res. 8, 271–276.

KHAN, P.K. (2005b), *Variation in dip-angle of the Indian plate subducting beneath the Burma plate and its tectonic implications*, Int. Geosci. J. 9, 227–234.

KHAN, P.K., and CHAKRABORTY, P.P. (2007), *The seismic b value and its correlation with Bouguer gravity anomaly over the Shillong plateau area: a new insight for tectonic implication*, J. Asian Earth Sci. 29, 136–147.

KHAN, P. K., GHOSH, M., and SRIVASTAVA, V.K. (2009), *Seismic a-value and the spatial stress-level variation in Northeast India*, J. Indian Geophys. Union 13, 49–62.

KHAN, P.K., MOHANTY, S., and MOHANTY, M. (2010), *Geodynamic implications for the 8 October 2005 North Pakistan earthquake*, Sur. Geophys. doi:10.1007/s10712-009-9083-1.

KIRBY, S.H., and KRONENBERG, A.K. (1987), *Rheology of the lithosphere: selected topics*, Rev. Geophys. 25, 1219–1244.

KLOOTWIJK, C.T., CANAGHAN, P.J., and POWELL, C.M. (1985), *The Himalayan arc large scale continental subduction, oroclinal bending and backarc spreading*, Earth Planet Sci Letts 75, 167–183.

KRISHNAN, M.S. (1960), *Geology of India and Burma*, Higgin− Bothams, Madras.

LE DAIN, A.Y., TAPPONNIER, P., and MOLNAR, P. (1984), *Active faulting and tectonics of Burma and surrounding regions*, J. Geophys. Res. 89, 453–472.

LOWRIE, W. (1997), *Fundamentals of Geophysics*, Cambridge Press.

MAUNG, H. (1987), *Transcurrent movements in the Burma-Andaman sea region*, Geol. 15, 911–912.

MEISSNER, R., and STREHLAU, J. (1982), *Limits of stresses in continental crust and their relationship to depth-frequency distribution for shallow earthquakes*, Tectonics 1, 73–89.

MITRA, S., PRIESTLEY, K., BHATTACHARYA, A.K., and GAUR, V.K. (2005), *Crustal structure and earthquake focal depths beneath northeastern India and southern Tibet*, Geophys. J. Int.160, 227–248.

MOGI, K. (1963), *The fracture of a semi-infinite body caused by an inner stress origin and its relation to earthquake phenomena*, Earthquake Res. Inst. Bull., Tokyo University 41, 595–614.

MOGI, K. (1967), *Regional variations in magnitude−frequency relation of earthquakes*, Earthquake Res. Inst. Bull., Tokyo University 5, 67−86.

MOLNAR, P. (1988), *Continental tectonics in the aftermath of plate tectonics*, Nature 335, 131–137.

MORI, J., and ABERCROMBIE, R.E. (1997), *Depth dependence of earthquake frequency-magnitude distributions in California: Implications for the rupture initiation*, J. Geophys. Res. 102, 15081–15090.

MUKHOPADHYAY, M. (1984), *Seismotectonics of transverse lineaments in the eastern Himalaya and its foredeep*, Tectonophysics 109, 227–240.

MUKHOPADHYAY, S., KHATTRI, K.N., and CHANDER, R. (1995), *Seismic velocity and related clastic parameters of the crust in the Shillong massif*, J. Him. Geol. 6, 1–8.

NANDY, D.R. (1980), *Tectonic patterns in north eastern India*, Indian J. Earth Sci. 7, 103–107.

NANDY, D.R., and DASGUPTA, S. (1986), Application of remote sensing in regional geological studies – a case study in northeastern part of India, *In* Proceeding of the International Seminar on Photogrammetry and Remote Sensing for Developing Countries, Survey of India, New Delhi, India, pp. T.4-P./6.1-T.4-P./6.4.

PACHECO, J.F., SCHOLZ, C.H., and SYKES, L.R. (1992), *Changes in frequency-size relationship from small to large earthquakes*, Nature 355, 71–73.

RADHA KRISHNA, M., and SANU, T.D. (2000), *Seismotectonics and rates of active crustal deformation in the Burmese arc and adjacent regions*, J. Geodyn. 30, 401–421.

RAI, S., PRAKASAM, K., and AGRAWAL, N. (1999), *Pn wave velocity and Moho geometry in northeastern India,* Proc. Indian Acad. Sci. (Earth Planet. Sci.) 108, 297–304.

RODGERS, J. (1987), *Chains of basement uplifts within cratons marginal to orogenic belts*, Am. J. Sci. 287, 661–692.

RUTTER, E.H., and BRODIE, K.H. (1992), *Rheology of the lower crust, In Continental Lower Crust*, Fountain, D.M., Arculus, R., and Kay, R.W. Eds., Elsevier, Amsterdam, pp. 201-267.

RYDELEK, P.A., and SACKS, I.S. (1989), *Testing the completeness of earthquake catalogues and the hypothesis of self-similarity*, Nature 337, 251–253.

SCHOLZ, C.H. (1968), *The frequency−magnitude relation of microfracturing in rock and its relation to earthquakes*, Bull. Seismol. Soc. Am. 58, 399–415.

SEEBER, L., ARMBRUSTER, J.G., and QUITTMEYER, R. (1981), *Seismicity and continental subduction in the Himalayan arc. In Zagros, Hindukush, Himalaya-Geodynamic Evolution, Geodynamics Series*, Gupta, H.K., and Delany, F.M., Eds., pp. 259–279.

STECKLER, M.S., AKHTER, S.H., and SEEBER, L. (2008), *Collision of the Ganges-Brahmaputra Delta with the Burma Arc: Implications for earthquake hazard*, Earth Planet. Sci. Lett. 273, 367–378.

TANDON, A.N. (1954), *Study of the great Assam earthquake of August, 1950 and its aftershocks*, Indian J. Met. Geophys. 5, 95–113.

THUSSU, J.L. (2002), *Geothermal Energy Resources of India*, Geological Survey of India, Lucknow, Spl. Pub. No. 69.

TSAPANOS, T.M. (1990), *b-values of two tectonic parts in the Circum-Pacific belt*, Pure Appl. Geophys. 134, 229–242.

UDIAS, A. (1999), *Principles of Seismology*, University Press, Cambridge, United Kingdom.

VERMA, R.K., MUKHOPADHYAY, M., and AHLUWALIA, M.S. (1976), *Seismicity, Gravity and Tectonics of Northeast India and Northern Burma*, Bull. Seismol. Soc. Am. 66, 1683–1694.

VERMA, R.K., and MUKHOPADHYAY, M. (1977), *An analysis of gravity field in North-eastern India*, Tectonophysics 42, 283–317.

WASON, H.R., SHARMA, M.L., KHAN, P.K., KAPOOR, K., NANDINI, D., and KARA, V. (2002), *Analysis of aftershocks of the Chamoli Earthquake of March 29, 1999 using broadband seismic data*, J. Him. Geol. 23, 7–18.

WATTS, A.B., and BUROV, E.B. (2003), *Lithospheric strength and its relationship to the elastic and seismogenic layer thickness*, Earth Planet. Sci. Lett. 213, 113–131.

WYSS, M. (1973), *Towards a physical understanding of the earthquake frequency distribution*, J. Royal Astron. Soc. Geophys. 31, 341–359.

WIEMER, S., and WYSS, M. (1997), *Mapping the frequency magnitude distribution in asperities: An improved technique to calculate recurrence times*, J. Geophys. Res. 102, 15115–15128.

WIEMER, S., and WYSS, M. (2000), *Minimum magnitude of completeness in earthquake catalogs: examples from Alaska, the Western United States, and Japan*, Bull. Seismol. Soc. Am. 90, 859–869.

WOESSNER, J., and WIEMER, S. (2005), *Assessing the quality of earthquake catalogues: estimating the magnitude of completeness and its uncertainty*, Bull. Seismol. Soc. Am. 95, 684–698, doi: 10.1785/0120040007.

(Received March 15, 2010, revised July 24, 2010, accepted July 27, 2010, Published online September 30, 2010)